# Electronic structure of the superconducting layered ternary nitrides $CaTaN_2$ and $CaNbN_2$

Josep M. Oliva,[1] Ruben Weht,[1,2] Pablo Ordejón,[1] and Enric Canadell[1]
[1]*Institut de Ciència de Materials de Barcelona (CSIC), Campus de la Universidad Autonoma de Barcelona, 08193 Bellaterra, Spain*
[2]*Departamento de Física, CNEA, Avenida General Paz y Constituyentes, 1650 San Martín, Argentina*
(Received 13 March 2000)

The electronic structure of the layered ternary nitrides $CaMN_2$ ($M=$ Ta, Nb) has been studied and the results are compared with those for the related $LiMoN_2$ phase. It is shown that the former are two-dimensional metals, with a Fermi surface very similar to that of the $1T$-$TaX_2$ ($X=$ S, Se) dichalcogenides, whereas the latter is a three-dimensional metal. The three phases show strong covalent bonding within the layers but ionic bonding with the alkali atom sheets.

The synthesis and structural characterization of binary nitrides owes very much to the pioneering work of Juza and co-workers.[1] Some of these materials have been found to possess interesting and useful properties. For instance, BN, AlN, and TaN have been extensively used as high temperature refractory ceramics and coatings, GaN and InN as semiconductors, etc. For a long time, progress beyond binary systems was slow because of considerable synthesis difficulties. However, solid state ternary transition-metal nitrides have received increased attention for the last ten years and new synthesis strategies have been developed. As a result, there is now a large and continuously growing list of ternary and higher-order transition-metal nitrides exhibiting very rich structural chemistry and physical properties.[2–5] Among them, the layered transition-metal nitrides seem to be specially important compounds. For example, the significant jump in the superconducting transition from $T_c=12$ K in the Li-doped layered nitride $\beta$-ZrNCl (Ref. 6) to 25 K in Li-doped $\beta$-HfNCl (Ref. 7) has recently called attention towards the still largely unexplored physics of layered transition metal nitrides.

Here we would like to discuss the electronic structure of $CaTaN_2$ and $CaNbN_2$,[5,8] two layered transition metal nitrides that have been reported to exhibit a superconducting transition at $\sim$8.2 K and $\sim$14 K, respectively.[5,8,9] The crystal structure of the two isostructural $CaMN_2$ ($M=$Nb,Ta) phases[8] consists of a series of $MN_2$ layers along the $c$ direction between which are hexagonal layers of $Ca^{2+}$ cations. The coordination environment of the $M$ atoms in the $MN_2$ layers is octahedral. The stacking of the successive $MN_2$ layers is such that the Ca atoms lie in the octahedral sites in between the N sublayers of two different $MN_2$ layers. With the usual oxidation states of $3-$ and $2+$ for N and Ca, respectively, the formal $d$-electron count for the $M$ atoms is $d^1$. Thus, the $TaN_2^{2-}$ layers of $CaTaN_2$ are isostructural and isoelectronic with the $TaX_2$ ($X=$S,Se) layers of $1T$-$TaX_2$,[10] two of the best studied and more interesting low-dimensional materials.[11] $CaTaN_2$ (like $CaNbN_2$) is apparently metallic but before entering into the superconducting state does not seem to exhibit any of the resistivity anomalies exhibited by the $1T$-$TaX_2$ phases.

At this point it is interesting to note the relationship between $CaTaN_2$ and $CaNbN_2$ with the layered nitride $LiMoN_2$.[12] This phase, which was the first metallic layered nitride, contains also $MN_2$ ($M=$Mo) layers between which are hexagonal layers of $Li^+$ cations. However, there is a major difference as compared to $CaTaN_2$: the coordination environment of the transition-metal atoms is trigonal prismatic instead of octahedral. With the usual oxidation states of $3-$ and $1+$ for N and Li, respectively, the formal $d$-electron count for the Mo atoms is also $d^1$. Thus, in the case of $LiMoN_2$ the $MoN_2^-$ layers are isostructural and isoelectronic with the $TaX_2$ ($X=$S,Se) layers of $2H$-$TaX_2$ ($X=$S,Se),[10] which also exhibit resistivity anomalies as a result of structural modulations.[13] However, the calculated Fermi surfaces for the two types of materials[14,15] are quite different and the magnetic susceptibility measurements for $LiMoN_2$ (Ref. 12) do not seem to provide any indication for the opening of gaps at the Fermi level.

The apparent absence of electronic instabilities in the above-mentioned nitrides despite the strong relationship with the $1T$- and $2H$-$TaX_2$ chalcogenides is interesting because it suggests that nitrides can have a distinctive physical behavior with respect to these strongly related materials. It could be argued that in $CaTaN_2$, $CaNbN_2$, and $LiMoN_2$ the $Li^+$ or $Ca^{2+}$ cations effectively couple the different layers in such a way that the nesting features in the Fermi surfaces of the $1T$- and $2H$-$MX_2$ phases are absent. We note, however, that the Fermi surface scenario has sometimes been challenged[16–18] as the origin for the resistivity anomalies of the $1T$- and/or $2H$-$MX_2$ phases (theoretical[14] and experimental[19] evidence seems to indicate that there is no nesting with the appropriate wave vectors in these compounds), so that the differences in physical behavior could well arise from differences in electronegativity, size, or polarizability of the nitride anions instead of variations in the Fermi surface. It is worthwhile noting that the $CaTaN_2$, $CaNbN_2$, and $LiMoN_2$ phases are part of a large group of layered compounds with the $AMN_2$ stoichiometry, which has received much attention recently.[3] In order to gain some insight into the electronic structure of these nitrides we report here on electronic structure calculations of the two superconducting layered nitrides $CaTaN_2$ and $CaNbN_2$.

The calculations reported here were performed applying the linearized augmented plane wave method (LAPW) that utilizes a fully general shape of density and potential. The WIEN code[20] has been used along this work. LAPW sphere radii of 1.9 a.u. for Ca, 2.0 a.u. for Ta/Nb, and 1.9 a.u. for N were chosen with cutoffs of $RK_{max}$ up to 9 (see Ref. 20), providing a well-converged basis set with more than 600

 

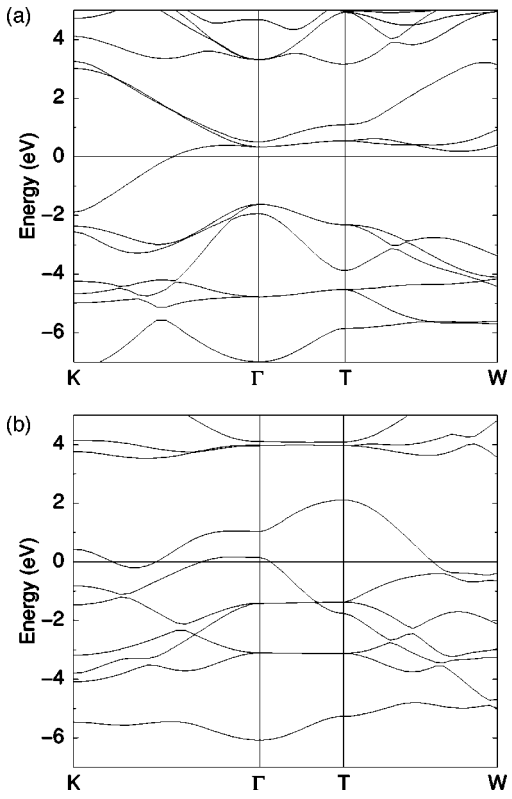


FIG. 1. Band structure for (a) $CaTaN_2$ and (b) $LiMoN_2$. $\Gamma=(0,0,0)$, $K=(1/2,1/2,0)$, $T=(1/2,1/2,1/2)$, and $W=(3/4,1/2,1/4)$ in units of the rhombohedral reciprocal lattice vectors. Note that the $\Gamma$-$T$ direction is along the threefold rhombohedral axis

functions per primitive cell. Self-consistency was carried out on $k$ points meshes of around 1000 points in the total Brillouin zone. Local orbitals were added to the basis set for extra flexibility and to allow semicore states to be treated within the same energy window as the band states. The generalized gradient approximation exchange correlation functional of Perdew *et al.*[21] was used.

Since the results for both of the $CaMN_2$ ($M=$Ta,Nb) phases were found to be almost identical, we will only report here those concerning $CaTaN_2$. Although the electronic structure of $LiMoN_2$ was already studied by Singh,[15] the same type of calculations for $LiMoN_2$ are also reported here, for comparative purposes. All calculations were carried out using the rhombohedral unit cell and experimental lattice constants (5.521 Å for $LiMoN_2$, 5.843 Å for $CaTaN_2$ and 5.846 Å for $CaNbN_2$).

The calculated band structure and the total and projected densities of states (DOS) for $CaTaN_2$ are shown in Figs. 1(a) and 2, respectively. Analysis of the eigenvectors for different points of the Brillouin zone as well as the projected densities of states of Fig. 2 show that the major components of the lowest six bands of Fig. 1(a) are localized on the nitrogen atoms whereas the next band is strongly tantalum-based. $CaTaN_2$ has a half-filled Ta-based band and should be metallic. Note that at the $\Gamma$ point the partially filled band is practically degenerate with two other Ta-based bands, a consequence of the very regular octahedral coordination for the Ta atoms. It is important to note that the band dispersion of the partially filled band along the $\Gamma$-T direction, i.e., along the rhombohedral axis, is practically nil. Since this direction

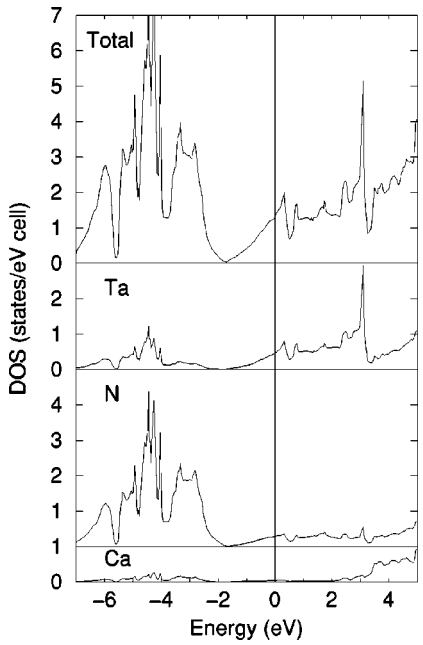


FIG. 2. Total and projected density of states of $CaTaN_2$ projected onto the Ca, N, and Ta sites.

is perpendicular to the $TaN_2$ layers, it is clear that, as far as the partially filled band is concerned, $CaTaN_2$ should be considered as a two-dimensional system. As can be seen in Fig. 2, Ca practically does not contribute to this band. Note, however, that the dispersion along the interlayer direction is quite sizable for some lower-lying bands of Fig. 1(a), which are thus more heavily based on the N atoms and consequently are better suited to lead to interlayer interactions either directly or through the Ca atoms. However, the Ca contribution to the occupied levels (see Fig. 2) is very small. The N($2p$) and Ta($5d$) states strongly hybridize above and below the minimum in the density of states around $-2$ eV. This suggests covalent bonding within the $TaN_2$ layers but ionic bonding between the layers and the Ca sheets.

We thus conclude that $CaTaN_2$ should be a two-dimensional metal, exactly as they are in the above-mentioned $1T$-$MX_2$ phases. This is confirmed by the calculated Fermi surface, which is shown in Fig. 3(a) in a plane perpendicular to the threefold rhombohedral axis. Note that starting from the $\Gamma$ point, as one proceeds along this axis the $T$ point is reached. Since the Fermi surface plot is very similar around the $\Gamma$ and $T$ points, the three-dimensional Fermi surface of this system is very easy to imagine: it is made of slightly warped tubes with a pseudo-elliptical section. We have verified this by calculating the Fermi surface in different sections perpendicular to the threefold axis. This Fermi surface does not exhibit nesting features so that it is understandable that, even if $CaTaN_2$ is a low-dimensional metal, it does not exhibit the usual resistivity anomalies shown by these systems. It is also interesting to note that our calculated Fermi surface is very similar to that for $1T$-$TaS_2$ for which the theoretical[14] and angle-resolved photoelectron spectroscopy[19] (ARPES) results are in excellent agreement. As noted by Pillo *et al.*[19] it is surprising that the ARPES mapping of the Fermi surface of $1T$-$TaS_2$ at room temperature, i.e., in the quasicommensurate charge density wave phase,

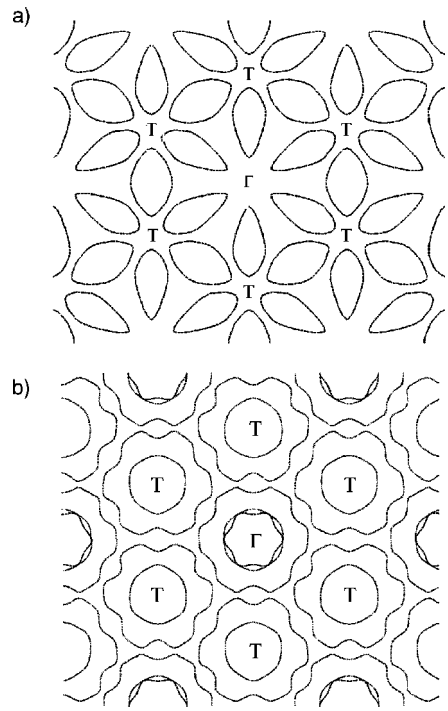


FIG. 3. Calculated Fermi surfaces for (a) $CaTaN_2$ and (b) $LiMoN_2$ in the plane perpendicular to the threefold axis.

does not exhibit the appropriate gap openings. These results suggest that, as proposed by previous theoretical studies,[17,18] local chemical bonding (i.e., ordered clusterization) but not Fermi surface nesting is at the origin of the charge density waves in $1T$-$TaS_2$. Then, why do $CaTaN_2$ and $CaNbN_2$ not seem to lead to this type of clusterization within their $MN_2$ layers? We believe that the smaller polarizability of the nitrogen atoms with respect to the chalcogens, the presence of the calcium cations in the octahedral sites in between the different $MN_2$ layers, and the shorter $M$-N distances altogether would lead to a too large a lattice strain for the metal-metal clusterization in the $CaMN_2$ ($M$=Ta,Nb) phases.

The band structure of $LiMoN_2$ [see Fig. 1(b)] exhibits interesting differences compared with that of $CaTaN_2$. The first six bands starting from the bottom of Fig. 1(b) are more heavily based on the nitrogen atoms, whereas the next one is more heavily based on the molybdenum. The important difference with the band structure of Fig. 1(a) is that now two bands are partially filled. The fact that one of the heavily-nitrogen-based bands is partially empty means that the nitrogen atoms must be considered in a $N^{(3-x)-}$ formal oxidation state and thus the $d$-electron count for Mo is $d^{1+x}$. Another important difference with the band structure of Fig. 1(a) is that the band dispersion of the two partially filled bands along the interlayer direction is quite important. The analysis of the band mixing among the formally nitrogen-based bands and the lowest of the molybdenum-based bands is somewhat involved and will not be discussed here. However, what is already clear just from simple inspection of Fig. 1(b) is that $LiMoN_2$ must be a three-dimensional metal. It is interesting to note that this fact does not result from interlayer coupling through the Li atoms because analysis of the wave vectors shows that the lithium atoms practically do not contribute to the partially filled bands (see also the detailed analysis in Ref. 15). $LiMoN_2$ is a three-dimensional metal because the lowest molybdenum-based band dips into the manifold of the nitrogen-based bands and thus overlaps and mixes in some character of the nitrogen bands that exhibit dispersion along the interlayer direction, mostly because of direct interlayer nitrogen-nitrogen interactions.

The three-dimensional metallic character of $LiMoN_2$ can be clearly seen in the Fermi surface shown in Fig. 3(b). In contrast to $CaTaN_2$, the Fermi surface around the $\Gamma$ and $T$ points is different: there are two closed lines around the $T$ point but three around $\Gamma$. This means that the inner closed loop around $\Gamma$ crosses the threefold rhombohedral axis between $\Gamma$ and $T$ and thus leads to a closed surface. In other words, the inner closed loop around $\Gamma$ in Fig. 3(b) leads to a three-dimensional contribution to the Fermi surface, whereas the other two lead to a pair of two-dimensional contributions. It is thus clear that the electronic structure of $LiMoN_2$ is very different from that of the apparently related $d^1$ $2H$-$MX_2$ phases. In view of the calculated Fermi surface, it is not expected that $LiMoN_2$ exhibits any low-temperature resistivity anomaly related to Fermi surface instabilities.

One of the more interesting results of our study is the fact that, depending on the nature and/or local coordination of the transition-metal atom, some of the transition-metal-based bands can dip into the manifold of the ligand-based bands. This fact, which although for different reasons was also noticed for layered transition-metal tellurides,[22] can be at the origin of very interesting structural and physical properties for transition-metal nitrides and thus gives additional interest to the study of this type of solids.

We are grateful to Professor H. Jacobs (Universität Dortmund) for making available the crystal structure data of $CaTaN_2$ and $CaNbN_2$. This work was supported by DGES-Spain (Project PB96-0859), Generalitat de Catalunya (1997 SGR 24), and Motorola PSRL. J.M.O. acknowledges the Ministerio de Educación y Cultura (Spain) for a contract of the Programa de Incorporación de Doctores y Tecnólogos. R.W. acknowledges support from Fundación Antorchas Grants No. A-13622/1-103 and No. A-13661/1-27. Part of the research has been done using the computing resources of CESCA and CEPBA, coordinated by C$^4$.

[1] R. Juza, Adv. Inorg. Chem. Radiochem. **9**, 81 (1966); R. Juza, K. Langer, and K. Von Benda, Angew. Chem. Int. Ed. Engl. **7**, 360 (1968).

[2] F. J. DiSalvo, Science **247**, 649 (1990).

[3] D. H. Gregory, J. Chem. Soc. Dalton Trans. **1999**, 259.

[4] R. Kniep, Pure Appl. Chem. **69**, 185 (1997).

[5] R. Niewa and H. Jacobs, Chem. Rev. **96**, 2053 (1996).

[6] S. Yamanaka, H. Kawaji, K. Hotehama, and M. Ohashi, Adv. Mater. **9**, 771 (1996).

[7] S. Yamanaka, K. Hotehama, and H. Kawaji, Nature (London) **392**, 580 (1998).

[8] T. Brokamp, Ph.d. dissertation, Universität Dortmund, 1991; C.

Wachsmann, Ph.d. dissertation, Universität Dortmund, 1995.
[9] V. Balbarin, R. B. van Dover, and F. J. DiSalvo, J. Phys. Chem. Solids **57**, 1919 (1996).
[10] F. Hulliger, *Structural Chemistry of Layer-Type Phases* (Reidel, Dordrecht, 1976).
[11] For some reviews see for instance, *Structure Phase Transitions in Layered Transition Metal Compounds*, edited by K. Motizuki (Reidel, Dordrecht, 1986); *Electronic Structure and Electronic Transitions in Layered Materials*, edited by V. Grasso (Reidel, Dordrecht, 1986); R. H. Friend and A. Yoffe, Adv. Phys. **36**, 1 (1987); R. L. Withers and J. A. Wilson, J. Phys. C **19**, 4809 (1986).
[12] S. H. Elder, L. H. Doerrer, F. J. DiSalvo, J. B. Parise, D. Guyomard, and J. M. Tarascon, Chem. Mater. **4**, 928 (1992).
[13] J. A. Wilson, F. J. DiSalvo, and S. Mahajan, Adv. Phys. **24**, 117 (1975); P. M. Williams in *Crystallography and Crystal Chemistry of Materials with Layered Structures*, edited by F. Levy (Reidel, Dordrecht, 1976), Vol. 2, p. 51.
[14] For a review of the electronic structure of layered transition-metal dichalcogenides see E. Doni and R. Girlanda in *Electronic Structure and Electronic Transitions in Layered Materials* (Ref. 11).
[15] D. J. Singh, Phys. Rev. B **46**, 9332 (1992).
[16] N. V. Smith, D. S. Kevan, and F. J. DiSalvo, J. Phys. C **18**, 3175 (1985).
[17] C. Haas, Solid State Commun. **26**, 709 (1978); J. Solid State Chem. **57**, 82 (1985).
[18] M.-H. Whangbo and E. Canadell, J. Am. Chem. Soc. **114**, 9587 (1992).
[19] Th. Pillo, J. Hayoz, H. Berger, M. Grioni, L. Schlapbach, and P. Aebi, Phys. Rev. Lett. **83**, 3494 (1999).
[20] P. Blaha, K. Schwarz, and J. Luitz, WIEN97 (Vienna University of Technology, Vienna, 1997). Improved and updated version of the original copyrighted WIEN code, which was published by P. Blaha, K. Schwarz, P. Sorantin and S. B. Trickey, Comput. Phys. Commun. **59**, 399 (1990).
[21] J. P. Perdew, K. Burke, and M. Ernzerhof, Phys. Rev. Lett. **77**, 3865 (1996).
[22] E. Canadell, S. Jobic, R. Brec, J. Rouxel, and M.-H. Whangbo, J. Solid State Chem. **99**, 189 (1992).